Research Article

SURFACE and INTERFACE ANALYSIS

Received: 24 March 2010 Revised: 3 June 2010 Accepted: 3 June 2010 Published online in Wiley Online Library: 27 July 2010

(wileyonlinelibrary.com) DOI 10.1002/sia.3658

Effect of repetition nanoindentation of GaN epilayers on *a*-axis sapphire substrates

Meng-Hung Lin,[a] Hua-Chiang Wen,[b]* Zue-Chin Chang,[b] Shyh-Chi Wu,[c] Wen-Fa Wu[d] and Chang-Pin Chou[a]

In this work, gallium nitride (GaN) epilayers were deposited on *a*-axis sapphire substrate by means of metal organic chemical vapor deposition (MOCVD). Berkovich nanoindentation was used to explore the repetition pressure-induced impairment of the GaN film. The observation of load-displacement vs stress-strain curves concludes that basal slip is implicated in the deformation on the A plane GaN. The increase in the hardness (*H*) and elastic modulus (*E*) was determined from cyclic nanoindentation, and resulted in a crack due to the formation of incipient slip bands and/or the to-and-fro motion of mobile dislocation. It is indicated that the generation of individual dislocation and residual deformation of the GaN films are showed by CL mapping analysis. From the morphological studies, it is revealed that the crack was found by means of atomic force microscope (AFM) technique at nine loading/reloading cycles even after the indentation beyond the critical depth on the residual indentation impression.

Keywords: gallium nitride; metal organic chemical vapor deposition; nanoindentation; atomic force microscopy

Introduction

Gallium nitride (GaN) is III-V wide-band-gap semiconductor and potential candidate for the realization of photonic devices in blue/green light emitting diodes (LED), semiconductor lasers, and optical detectors.[1] GaN involves the wide-band-gap, high breakdown field and high electron saturation velocity, which make GaN to play a great role in the development of electronic devices operating at high temperature, high power and high frequency relative to competing materials (silicon and gallium arsenide).[2,3] In terms of GaN film, the mismatch of lattice constants and thermal expansion coefficients in this heteroepitaxy serve high dislocation densities and high level of residual strain in the postgrowth of thin film, which affects its mechanical properties, etc.[4–7] The mechanical damages of GaN films, such as film cracking and interface delamination caused by thermal stresses and chemical–mechanical polishing, usually suppress the processing yield and application reliability of microelectronic devices. In this scenario, to access accounting precisely in the mechanical properties of GaN remains a challenge. It has been made to develop processes to grow thick GaN films, and subsequently, separate them from their substrates as evidenced.[8–12] Notice that, GaN film on sapphire substrates exhibits large lattice mismatch (about 13.9%) causing in-plane tensile strain in the GaN film. The most common orientation of sapphire used for GaN is the *c*-axis sapphire. In fact, the lattice mismatch of the GaN film on *a*-axis ($11\bar{2}0$) sapphire is less (2%) than that on *c*-axis (0001) sapphire (13.9%), which promises for excellent quality of GaN growth with improved surface morphology.[13]

Above them, compared to bulk, single crystals and the deformation mechanism of the films can serve to highly correlate to the geometrical dimensions and the materials defect structure. The misfit dislocations at the interface of GaN films, however, can play an important role of carrier mobility and luminescence efficiency, etc. As a consequence, nanoindentation has proven to be a powerful tool for probing the information on the mechanical properties of GaN films with characteristic dimensions in the submicron regime, such as hardness and Young's modulus.[14,15] In terms of indentation load on GaN films, the nanoindentation-induced discontinuity in the load-displacement curve has been revealed. The slip-band movement[16,17] and dislocation nucleation mechanism,[14][18] to explain this pop-in event on *c*-axis GaN epilayers or bulk single crystals have been investigated.[19] In our prior article, the proposal of *a*-axis GaN films had been attempts in pop-in study,[20] but for reasons that are unclear from repetition pressure-induced impairment events.

In this paper, we apply the nanoindentation technique to understand the response of GaN surfaces to a localized stress. The pressure-induced impairment of GaN films/*a*-axis sapphire substrate has been investigated by using nanoindentation, atomic force microscope (AFM) and cathodoluminescence (CL) mapping. A significant investigation of the mechanical characterizations on GaN films is motivated here.

* *Correspondence to: Hua-Chiang Wen, Department of Mechanical Engineering, Chin-Yi University of Technology, Taichung 411, Taiwan. E-mail: a091316104@gmail.com*

a *Department of Mechanical Engineering, National Chiao Tung University, Hsinchu 300, Taiwan*

b *Department of Mechanical Engineering, National Chung Hsing University, Taichung 40227, Taiwan*

c *Chung Shan Institute of Science and Technology, CSIST, Taoyuan 325, Taiwan, ROC*

d *National Nano Device Laboratories, Hsinchu 300, Taiwan*

SURFACE and INTERFACE ANALYSIS

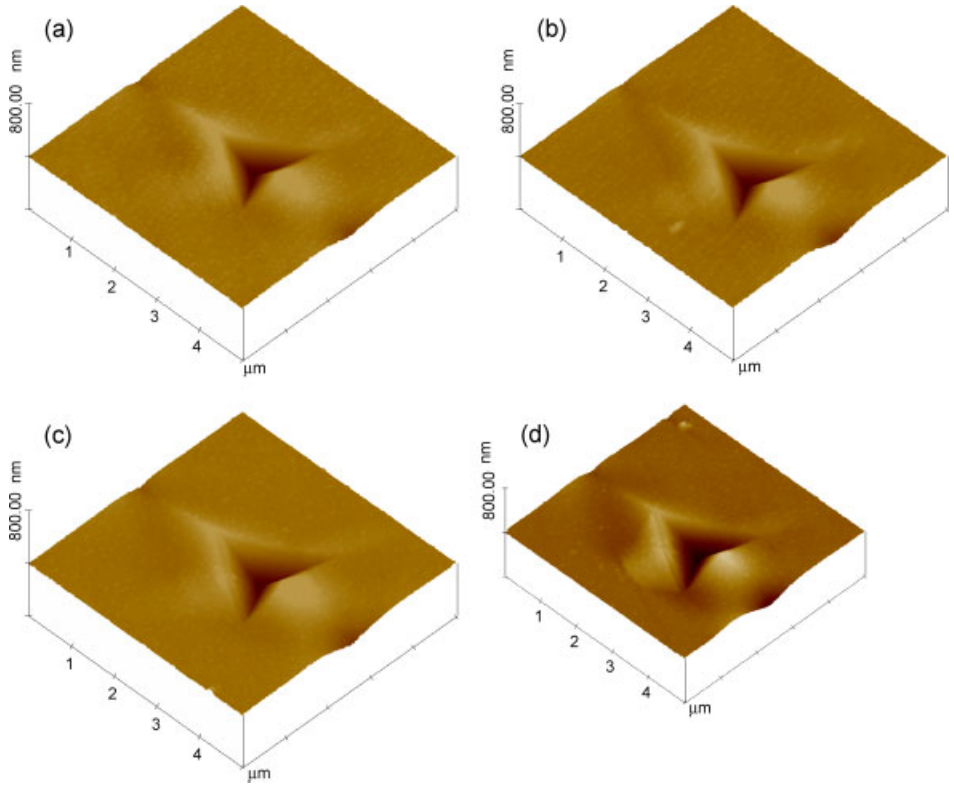

Figure 1. AFM images of indented GaN film/*a*-axis sapphire surfaces: (a) typical, (b) three, (c) six and (d) nine loading/reloading cycles, respectively.

Experimental

The GaN films used in this study was grown on *a*-axis ($11\bar{2}0$) sapphire plane substrates by using the metal-organic chemical vapor deposition (MOCVD) method. To fabricate the GaN films, a 10-nm-thick AlN-buffer layer was first grown on *a*-axis ($11\bar{2}0$) sapphire substrate. Then, GaN films with a thickness of close to 2 µm was grown on top of the buffer layer by MOCVD at 1100 °C, using Triethylgallium (TEGa), trimethylaluminium (TMAl), and ammonia (NH_3) as the gallium, aluminium and nitrogen, respectively.

The mechanical properties of GaN films performed by a Nanoindentation system (Nano Indenter XP instrument, MTS Corporation, Nano Instruments Innovation Center, TN, USA) with Berkovich indenter tip, whose radius of curvature is 50 nm, were conducted under force contact stiffness measurement (FSM) technique with repetition pressure-induced impairment at the constant load of 25 mN. In FSM measurement, each indentation location was separated by 30 µm in order to avoid possible interference between neighboring indents. Here, all indents were performed at room temperature. The analytic method developed by Oliver and Pharr was adopted to determine the hardness (*H*) and Young's modulus (*E*) of the GaN films from the load-displacement curves.[21] The thermal drift was kept below ±0.05 nm/s for all indentations considered in this work. The nanoindentation-induced crack morphology of the GaN films was examined by tapping mode atomic force microscopy (AFM, Veeco D5000). In addition, cathodoluminescence (CL) mapping acquired at a wavelength of 550 nm from an indented GaN films indented was characterized using a CL apparatus (HORIBA Co., Ltd.). The room-temperature CL measurements were performed using a JEOL JSM-7001F field emission scanning electron microscope. An electron beam energy of 20 keV was selected to excite the GaN surface. The CL light was dispersed by a 2400 nm grating spectrometer and detected by a liquid N_2-cooled charge-coupled device.

Results and Discussion

In term of indentation, residual impression of repeated indent mark was examined by tapping mode 3D-AFM to check for the evidence of slip, cracking, and pile-up/sink-in phomenon. Shown in Fig. 1 are typical amplitude-mode AFM images of a (a) typical cycle, (b) three, (c) six and (d) nine loading/reloading cycles to maintain a maximum load of 25 mN. In Fig. 1(a), the AFM image clearly illustrates that slight activation of the pyramidal slip near the indent mark, which occurs at typical cycle nanoindentation, is suppressed in the GaN films. A comparison of three and six loading/reloading cycles nanoindentation images (Fig. 1(b) and (c)) gives a gradation of protrusion that means some pyramidal slip nucleation, rather than that of typical cycle one. It is suggested that the slip mechanism can be responsible for the pile-up events during the loading of GaN. Furthermore, the AFM image of the residual indentation mark at nine loading/reloading cycles reveals the pyramidal slip and partial crack (Fig. 1(d)). The dislocation-induced 'pop-in' event tends to be associated with two distinct deformation behaviors before (pure elastic behavior) and after (elastoplastic behavior) the phenomenon. The hardness (*H*) and elastic modulus (*E*) as a function of indentation depth can be obtained from the FSM measurements; for the measured results of the GaN films/A plane sapphire substrate, *H* were 16.4 ± 0.2, 15.6 ± 0.1, 16.6 ± 0.2, 26.5 ± 0.8 GPa, while *E* were 409.7 ± 12, 400.7 ± 11, 383.5 ± 9, 758.8 ± 18 GPa, respectively. The soft GaN

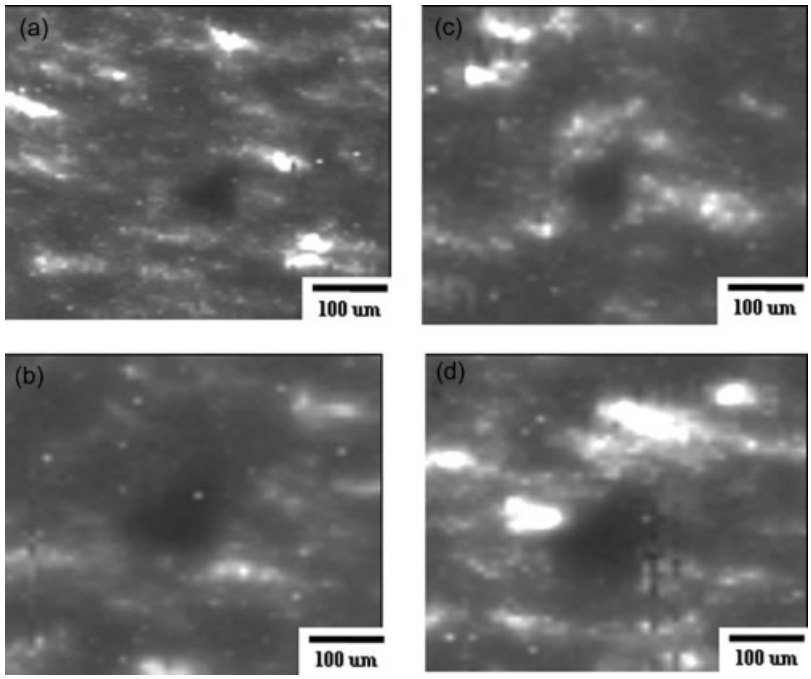

Figure 2. The CL mapping acquired at a wavelength of 550 nm from an indented GaN films: (a) typical, (b) three, (c) six and (d) nine loading/reloading cycles, respectively.

films was grown epitaxially on a hard sapphire substrate, it tends to find that the differences in lattice parameters and thermal expansion coefficients between the film and substrate. It may introduce a misfit strain at the interface, and the strain is released by generating threading dislocations in the GaN epilayers.[22,23] From the plane view of the indentation mark, Fig. 1 shows the residual volume from the edge of indentation. There is massive material transfer from below the indented zone to the sides of the indentation mark. Navamathavan *et al*.[24] revealed the residual impression of the indentation mark by Berkovich indenter tip. The pile-up event on the morphological surface is clearly the observation from SEM technique. Barsoum *et al*. also reported[25] that pop-in events and the cracks under a Berkovich indenter were observed. While the indenter suddenly penetrates into the basal planes, they must rupture (Fig. 1(d)). Since the rupture is associated with the repeated indenter cycles, the relatively large displacements at low stresses below the bend are most probably related to the back and forth motion of delamination. It is believed that the discrepancies in the mechanical parameters obtained by repeated indentation methods are mainly due to the specific tip–surface contact configuration and stress distribution inherent in the system of GaN films/*a*-axis sapphire.

In Fig. 2, the CL mappings acquired at a wavelength of 550 nm from a GaN films indented were presented at (a) typical, (b) three, (c) six and (d) nine loading/reloading cycles, respectively. These CL images reveal the distribution of indentation-induced extended defects; the cube-corner indenter form and these extended defects reflect some of the radial symmetry of the stress field (Fig. 2(a–c)). In contrast, another luminescence/topography distribution CL image revealed a crack line that formed after nine loading/reloading cycles (Fig. 2(d)). Slip enhancement may contribute to the crack that can be observed during loading/reloading and, the mechanism may be due to the plastic deformation.[15] In the GaN films, the indented area below the propagation of dislocations is observed by CL image that also revealed a detectable reduction in the intensity of the CL emission.[26–33] In the case of six loading/reloading cycles, only a small percentage of indentations was plastically deformed (Fig. 2(c)). CL imaging could distinguish between the indentations that had undergone several degree of plastic deformation, which location was purely in the elastic regime (Fig. 2(d)). As a result, we detected an observable CL impression only after the pile-up event, providing convincing evidence that the phenomenon involves the nucleation of slip as the deformation mode.

Above them, the load-indentation behaviors for the GaN films on the A plane sapphire is revealed in Fig. 3. At the beginning, the FSM serves the typical load vs penetration depth of GaN film (Fig. 3(a)). After the three cycles, the load vs penetration depth of GaN film is recorded; the repetition pressure-induced curve means gradual elastic deformation. The repetition pressure induced under three and six loading/reloading cycles nanoindentation images (Fig. 3(b) and (c)) leads to more strain hardening compared with that of a typical one (Fig. 3(a)). It is noted that the strain hardening is consistent with the decrease in the penetration depth. While Fig. 3(d) is superimposed, it becomes evident that the crack and the increased penetration depth are almost identical at CL imaging (Fig. 2(d)). Barsoum *et al*.[15] noted that all slips are basal and the stress-strain curves both before and after the pop-ins for both C and A orientations, presumably, were almost perfectly superimposable in sapphire. It is thus reasonable to implicate basal slip for the deformation in the A orientation. We concluded that the corresponding penetration depth vs repetition cycles in Fig. 4 and the strain hardening of GaN films partially induced as the penetration depth are observed to decrease not only from typical to six loading/reloading cycles, but also nine loading/reloading cycles. Consequently, the system (GaN films/*a*-axis sapphire) can be interacted by indenter tip to appear in the deformed zone, the threading dislocations then excursion into films through certain depths, afterward causing the pop-in event. It is conjectured that the mechanism of the event is caused by slip bands,[27–29]

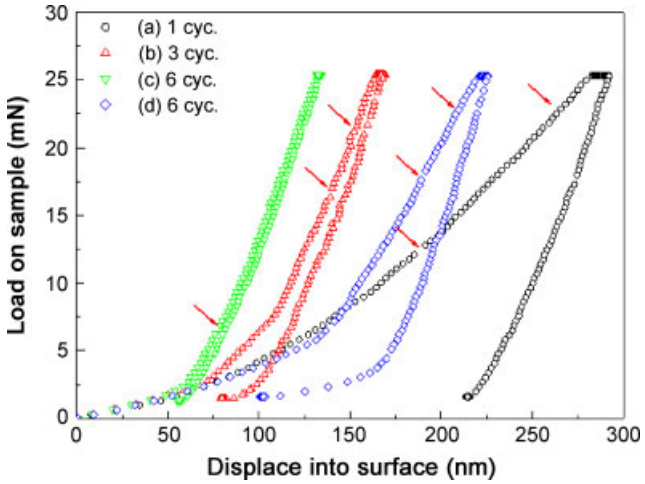

Figure 3. The typical load vs penetration depth curve of GaN film: (a) typical, (b) three, (c) six and (d) nine loading/reloading cycles, respectively.

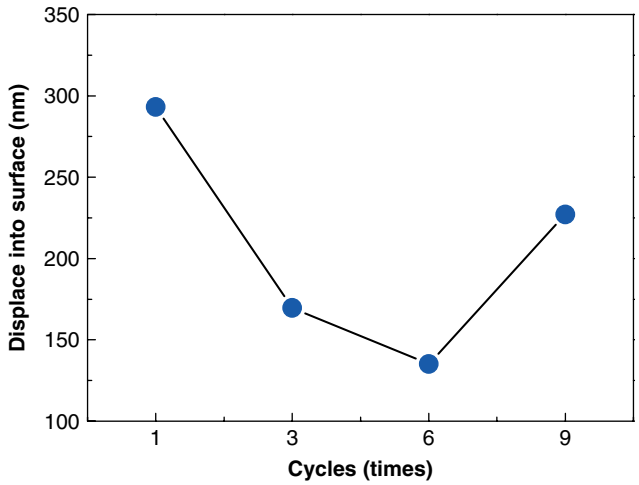

Figure 4. The penetration depth vs loading/reloading of GaN film: (a) typical, (b) three, (c) six and (d) nine loading/reloading cycles, respectively.

and/or dislocation nucleation.[30] However, the inner failure of the GaN films is observed while a crack suddenly occurrs at the condition of nine loading/reloading cycles. It is speculated that the repetition pressure-induced impairment during loading were contributed by the multiple pop-in events, and can be revealed over the indentation load and penetration depth.[20,24] From the previous report,[15,31–32], they discussed the deformation mechanisms in freestanding films. The successive indentations in the same location generated a series of hysteresis loops in which the first loop was slightly open, but subsequent loops were perfectly superimposable. For this case, the investigation of initial deformation of GaN films is measured under cyclic nanoindentation, which films deformed elastically and residual deformation is observed. This leads to larger deviations in the penetration depth vs cyclic nanoindentation. The mechanisms responsible for the dislocation recovery appear to be associated with the activation of dislocation sources brought about by loading-unloading cycle of the nanoindentation tip upon GaN films. The plastic deformation prior to loading-unloading cycle is associated with the individual movement of a small number of new nucleation, and large shear stress is quickly accumulated underneath the indenter tip. When the local stress underneath the tip reaches high level cycles, a burst of collective dislocation movement on the slip systems is activated, resulting in a release of local stress. The extensive interactions between the dislocations slipping along the GaN surface, therefore, confined the slip bands resulting in a pop-in event due to the deformed and strain-hardened lattice structure. It is suggested that the primary deformation mechanism of the GaN films may be due to dislocation nucleation and propagation along the easy slip systems.

Conclusion

We employed a combination of nanoindentation and AFM techniques to investigate the cyclic nanoindentation deformation behaviors of the GaN films/*a*-axis sapphire substrate. From AFM scans, the pop-ins resulted in impressions with depths that corresponded to the extent of residual penetration, or plastic deformation, registered in the first cycle. A material pile-up was also seen around the impressions.

The deformation mechanisms of the GaN films were observed in the form of a pop-in event during loading-unloading cycle, especially leading to deviations in the penetration depth vs cyclic nanoindentation loading/unloading. A CL images study of the indentation impressions show the clear evidence on the observation of the defects transform. In addition, the transformation of strain hardening of GaN is occurred under the cyclic nanoindenter test. The strain energy is transformed to mobile dislocation and resulted in a pop-in event initially. It is speculated that the repetition pressure-induced impairment was contributed by the multiple pop-in events, and are revealed over the indentation load and penetration depth.

Acknowledgements

This research was supported by the National Science Council of the Republic of China under Contract NSC-98-2221-E-009-069, and by the National Nano Device Laboratories in Taiwan under Contract NDL97-C04SG-088 and NDL97-C05SG-087.

References

[1] S. J. Pearton, J. C. Zolper, R. J. Shul, F. Ren, *J. Appl. Phys.* **1999**, *86*, 1.
[2] S. J. Pearton, F. Ren, A. P. Zhang, G. Dang, X. A. Cao, K. P. Lee, *Mater. Sci. Eng., B* **2001**, *82*, 227.
[3] C. H. Oxley, *Solid-State Electron.* **2004**, *48*, 1197.
[4] F. A. Ponce, D. P. Bour, *Nature* **1997**, *386*, 351.
[5] S. Nakamura, T. Mukai, M. Senoh, *J. Appl. Phys.* **1994**, *75*, 8189.
[6] T. Nagatomo, T. Kuboyama, H. Minamino, O. Omoto, *Jpn. J. Appl. Phys.* **1989**, *28*, L1334.
[7] N. Yoshimoto, T. Matsuoka, T. Sasaki, A. Katsui, *Appl. Phys. Lett.* **1991**, *59*, 2251.
[8] L. Liu, J. H. Edgar, *Mater. Sci. Eng., R* **2002**, *37*, 61.
[9] H. M. Kim, J. E. Oh, T. W. Kang, *Mater. Lett.* **2001**, *47*, 276.
[10] K. Motoki, T. Okahisa, S. Nakahata, A. Matsumoto, H. Kimura, H. Kasai, *Mater. Sci. Eng., B* **2002**, *93*, 123.
[11] R. P. Vaudo, G. R. Brandes, J. S. Flynn, X. Xu, M. F. Chriss, C. S. Christos, D. M. Keogh, F. D. Tamweber, IWN 2000, *IPAP ConferenceSeries C1*, 15, **2000**, Nagoya, Japan.
[12] Y. Oshima, T. Eri, M. Shibata, H. Sunakawa, K. Kaboyashi, T. Ichihashi, A. Usui, *Jpn. J. Appl. Phys.* **2003**, *42*, L1.
[13] L. Liu, J. H. Edgar, *Mater. Sci. and Eng., R* **2002**, *37*, 61.
[14] R. Nowak, M. Pessa, M. Suganuma, M. Leszczynski, I. Grzegory, S. Porowski, F. Yoshida, *Appl. Phys. Lett.* **1999**, *75*, 2070.

[15] S. Basu, M. W. Barsoum, A. D. Williams, T. D. Moustakas, *J. Appl. Phys.* **2007**, *101*, 083522.
[16] S. O. Kucheyev, J. E. Bradby, J. S. Williams, C. Jagadish, M. V. Swain, G. Li, *Appl. Phys. Lett.* **2001**, *78*, 156.
[17] S. O. Kucheyev, J. E. Bradby, J. S. Williams, C. Jagadish, M. Toth, M. R. Phillips, M. V. Swain, *Appl. Phys. Lett.* **2000**, *77*, 3373.
[18] D. Caceres, I. Vergara, R. Gonzalez, E. Monroy, F. Calle, E. Munoz, F. Omnes, *J. Appl. Phys.* **1999**, *86*, 6773.
[19] T. Wei, Q. Hu, R. Duan, J. Wang, Y. Zeng, J. Li, Y. Yang, Y. Liu, *Nanoscale Res. Lett.* **2009**, *4*, 753.
[20] M. H. Lin, H. C. Wen, C. Y. Huang, Y. R. Jeng, W. H. Yau, W. F. Wu, C. P. Chou, *Appl. Sur. Sci.* **2010**, *256*, 3299.
[21] W. C. Oliver, G. M. Pharr, *J. Mater. Res.* **1992**, *7*, 1564.
[22] X. J. Ning, F. R. Chien, P. Pirouz, J. W. Yang, M. Asif Khan, *J. Mater. Res.* **1996**, *11*, 580.
[23] B. N. Sverdlov, G. A. Martin, H. Morkoc, D. J. Smith, *Appl. Phys. Lett.* **1995**, *67*, 2063.
[24] R. Navamathavan, Y. T. Moon, G. S. Kim, T. G. Lee, J. H. Hahn, S. J. Park, *Mater. Chem. Phys.* **2006**, *99*, 410.
[25] M. W. Barsoum, A. Murugaiah, S. R. Kalidindi, Y. Gogotsi, *Carbon* **2004**, *42*, 1435.
[26] J. E. Bradby, S. O. Kucheyev, J. S. Williams, J. W. Leung, M. V. Swain, P. Munroe, G. Li, M. R. Phillips, *Appl. Phys. Lett.* **2004**, *80*, 383.
[27] S. O. Kucheyev, J. E. Bradby, J. S. Williams, C. Jagadish, M. V. Swain, G. Li, *Appl. Phys. Lett.* **2001**, *78*, 156.
[28] S. O. Kucheyev, J. E. Bradby, J. S. Williams, C. Jagadish, M. Toth, M. R. Phillips, M. V. Swain, *Appl. Phys. Lett.* **2000**, *77*, 3373.
[29] J. E. Bradby, S. O. Kucheyev, J. S. Williams, J. W. Leung, M. V. Swain, P. Munroe, G. Li, M. R. Phillips, *Appl. Phys. Lett.* **2002**, *80*, 383.
[30] R. Nowak, M. Pessa, M. Suganuma, M. Leszczynski, I. Grzegory, S. Porowski, F. Yoshida, *Appl. Phys. Lett.* **1999**, *75*, 2070.
[31] M. W. Barsoum, A. Murugaiah, S. R. Kalidindi, T. Zhen, *Phys. Rev. Lett.* **2004**, *92*, 255508.
[32] S. Basu, M. W. Barsoum, S. R. Kalidindi, *J. Appl. Phys.* **2006**, *99*, 063501.
[33] S. R. Jian, I. J. Teng, J. M. Lu, *Nanoscale Res. Lett.* **2008**, *3*, 158.